Importance of Perfusion in Myocardial Viability Studies Using Delayed Contrast-Enhanced Magnetic Resonance Imaging

Erik Hedström,[a] Håkan Arheden,[a] Rolf Eriksson,[b] Lars Johansson,[b] Håkan Ahlström,[b] Tomas Bjerner[b]

[a] *Department of Clinical Physiology, Lund University, Lund, Sweden*
[b] *MR Unit, Department of Radiology, Uppsala University, Uppsala, Sweden*

Abstract

PURPOSE: To investigate whether an extracellular gadolinium-(Gd)-based contrast agent (CA) enters nonperfused myocardium during acute coronary occlusion, and whether nonperfused myocardium presents as hyperintense in delayed contrast-enhanced (DE) MR images in the absence of CA in that region.

MATERIALS AND METHODS: The left anterior descending coronary artery (LAD) was occluded for 200 minutes in six pigs. The longitudinal relaxation rate (R_1) in blood, perfused myocardium, and nonperfused myocardium was repeatedly measured using a Look-Locker sequence before and during the first hour after administration of Gd-DTPA-BMA.

RESULTS: While blood and perfused myocardium showed a major increase in R_1 after CA administration, nonperfused myocardium did not. R_1 in nonperfused myocardium was significantly lower than in blood and perfused myocardium during the first hour after CA administration. When the signal from perfused myocardium was nulled, demarcation of the hyperintense nonperfused myocardium was achieved in all of the study animals.

CONCLUSION: Gd-DTPA-BMA does not enter ischemic myocardium within one hour after administration during acute coronary occlusion. The ischemic region with complete absence of CA still appears bright when the signal from perfused myocardium is nulled using inversion-recovery DE-MRI. This finding is important for understanding the basic pathophysiology of inversion-recovery viability imaging, as well as for imaging of acute coronary syndromes.

Key words: myocardial viability; myocardial perfusion; myocardial infarction; ischemia; magnetic resonance imaging

Address reprint requests to: E.H., Department of Clinical Physiology, Lund University Hospital, SE-221 85 Lund, Sweden. E-mail: erik.hedstrom@med.lu.se

Introduction

Delayed contrast-enhanced (DE) MRI has become an established method to assess myocardial infarction in patients.[6,12,14,18] This imaging technique relies on R_1 ($1/T_1$) differences between infarcted and viable perfused myocardia after administration of an extracellular gadolinium-(Gd)-based contrast agent (CA). The contrast between infarcted and viable myocardia is enhanced using an inversion recovery sequence.[1,12,18,23,25,28] For this sequence the inversion time (TI) is set to null the signal from perfused myocardium, which then becomes black in the image while the infarcted myocardium becomes hyperintense (enhanced). It has been suggested that enhancement of infarcted myocardium may be due to higher concentrations of extracellular CA in this region, caused by delayed wash-in and wash-out kinetics[9,15,17,20] as well as to different distribution volumes[1,18,24,28] between infarcted and viable perfused myocardia. Furthermore, it has been shown that extracellular Gd-based MR CAs do not bind to the injured myocardium, and therefore binding does not contribute to the effect of late enhancement.[8]

Several studies[5,10,13,19,21,30] have indicated the importance of flow in delivering the CA into injured myocardium. However, DE-MRI studies have suggested that extracellular Gd-based CAs may diffuse into injured myocardium within one hour after administration.[9,15,17]

Therefore, the aim of the present study was to investigate whether an extracellular Gd-based CA enters nonperfused myocardium, and whether the nonperfused myocardium presents as hyperintense in DE-MR images also in the absence of CA in that region. Toward that end, we chose to use an in vivo experimental model of coronary occlusion with no collateral flow.[2,26]

Materials and Methods

Study protocol

The protocol and procedures were approved by the local Ethics Committee for Animal Experiments, in accordance with the guidelines from National Institutes of Health. Six Swedish farm pigs of both sexes with a weight of 31 ± 5 kg (26 to 40 kg) were used in the present study.

The pigs were sedated and anesthetized with intramuscular (i.m.) zolazepam-tiletamine (6 mg/kg) and i.m. xylazine (2.2 mg/kg) followed by 20 mg of morphine administered through an ear vein. They were tracheotomized and ventilated using a ventilator (Siemens-Elema servo ventilator 900C; Siemens-Elema, Solna, Sweden). The pigs were also fitted with catheters in one of the carotid arteries and one of the femoral arteries, in both ear veins and in one jugular vein. Anesthesia was maintained by continuous infusion of ketamine (20 mg/kg/h) and morphine

(0.48 mg/kg/h). Pancuronium bromide (6 mg) was given for muscle relaxation when necessary.

Myocardial ischemia was induced by permanent occlusion of the left anterior descending coronary artery (LAD) using a catheter with an inflatable balloon used for percutaneous coronary intervention (PCI). The animals underwent MRI 200 minutes after occlusion.

After MRI, persistent occlusion of the LAD was verified by repeating the x-ray angiography. The perfused myocardium was delineated by administration of 2 ml fluorescein in the jugular vein. The heart was allowed to beat for 30 seconds in order to guarantee uniform staining of perfused myocardium, and the animals were then euthanized by administration of potassium chloride. The heart was excised and cut at the same short-axis level used for imaging. The injured myocardium was visualized by immersion in 1 % triphenyltetrazolium chloride (TTC) at 37 ° C until staining occurred, approximately 15 minutes.[11]

MRI

All imaging was performed with the animals in the supine position during free breathing without respiratory compensation on a 1.5 T Gyroscan Intera system (Philips Medical Systems, Best, the Netherlands) using a 20-cm circular receive-only surface coil and triggering with a vectorcardiogram. R_1 measurements were performed in a short-axis midventricular view at the location of the nonperfused myocardium. Data was acquired using a single slice Look-Locker[7] sequence at baseline prior to administration of Gd-DTPA-BMA at a dose of 0.2 mmol/kg, and followed by 13 acquisitions during one hour. Each acquisition was collected over four minutes and 40 seconds. A nonselective inversion pulse was followed by 70 slice-selective excitation pulses starting at a TI of 14 ms with an increment of 42 ms between excitations, yielding 70 data points on the modulus inversion recovery curve.

The scan parameters were TE = 2.0 ms, flip angle = 6°, field of view = 300 mm, voxel size = $1.2 \times 2 \times 10$ mm, and acquisition matrix = 154×256 pixels. TI ranged from 14 ms to 2 912 ms. The time between inversion pulses was approximately three seconds. The distance from the apex to the short-axis slice was measured in a diastolic long-axis view for later slicing and staining of the myocardium.

MR image evaluation

Quantitative analysis of the data in the dynamic Look-Locker series was performed using dedicated software (DimView, by Atle Bjørnerud, Rikshospitalet University Hospital, Oslo, Norway). Parametric R_1 maps and corresponding

χ^2 error maps[4] (Figure 1) were calculated from a nonlinear least-squares fit of the Look-Locker data to the equation

$$SI(TI) = \beta|(1 - 2e^{-R_1 TI})| + K$$

where $||$ denotes the modulus, β and K are fitting constants and $R_1 = 1/T_1$ is the model parameter to be determined.[3]

R_1 was measured at each time-point in the left ventricular (LV) blood pool and in perfused and nonperfused myocardia. The size of the measured region of interest (ROI) was 188 ± 67 mm^2, 38 ± 15 mm^2, 27 ± 7 mm^2, in blood, perfused myocardium, and nonperfused myocardium, respectively, without including visual artifacts or edges of myocardium. The χ^2 error map was used to guide positioning of the ROI to avoid pixels that move between regions during the cardiac cycle. The standard deviation (SD) of R_1 was used as a control to avoid regions with high noise. The measured R_1 values were normalized to the baseline value (before CA administration) in each animal for comparison between regions and animals. For each time point after CA adminstration, ΔR_1 was defined as the difference between R_1 at that time point ($R_{1,\text{time}}$) and R_1 before CA administration ($R_{1,\text{baseline}}$).

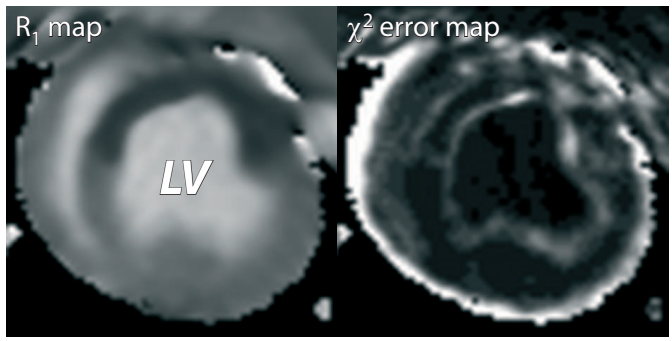

FIGURE 1 Parametric R_1 map (**left**) and corresponding χ^2 error map (**right**) that reflects the relative error in the curve fit. High signal intensity in the χ^2 error map indicates regions with poor curve fit due to cardiac motion. These regions were avoided for the measurements.

The intensity of the nonperfused myocardium was visually evaluated in images where TI was chosen to null the signal from perfused myocardium, as performed using DE-MRI.

Statistical analysis

The data were considered to consist of simple random samples from a normally distributed population, and a t-distribution was assumed to calculate the 95 % confidence interval (CI). Statistical significance was determined when the 95 % CIs did not overlap. Values are expressed as the mean ± SD.

Results

After CA administration, a major increase in R_1 was found for blood and perfused myocardium, but not for nonperfused myocardium. The relationships between R_1 values were similar in all animals. An example is shown in Figure 2A.

During the first hour after CA administration, a continuous decline was found for ΔR_1 in blood and perfused myocardium, whereas no significant change was found for nonperfused myocardium, indicating an absence of CA in nonperfused myocardium (Figure 2B). Moreover, ΔR_1 in nonperfused myocardium remained significantly lower than in blood and perfused myocardium throughout the measurement period (Figure 2B).

Demarcation of the hyperintense nonperfused myocardium was acheived in all animals when the signal from perfused myocardium was nulled (Figure 3B).

X-ray angiography and fluorescein showed persistent occlusion after MRI (Figure 4), and TTC showed changes indicative of myocardial infarction in all animals.

It was noted that before administration of CA, R_1 was higher in perfused myocardium than in nonperfused myocardiummyocardium, and was higher in nonperfused myocardium than in blood in all of the animals (Figure 5).

Discussion

The results of the present study indicate that no significant amount of Gd-DTPA-BMA enters nonperfused myocardium in vivo within one hour after CA administration in a model of coronary artery occlusion with no collateral flow. Furthermore, in DE-MRI, nonperfused myocardium becomes hyperintense—not because of an increased distribution volume of CA, but because of the complete absence of CA in this region.

The R_1 measurements in perfused myocardium before CA administration ($R_1 = 912 \pm 55$ ms^{-1}) are consistent with previous studies in which R_1 was found to be 850 ms^{-1} and 930 ms^{-1} in pig,[4,27] and 840 ms^{-1} in humans.[29]

The trend toward increased ΔR_1 in nonperfused myocardium 50–60 minutes after CA administration might increase even more if it was followed for a longer time. However, imaging of injured myocardium is usually performed optimally at

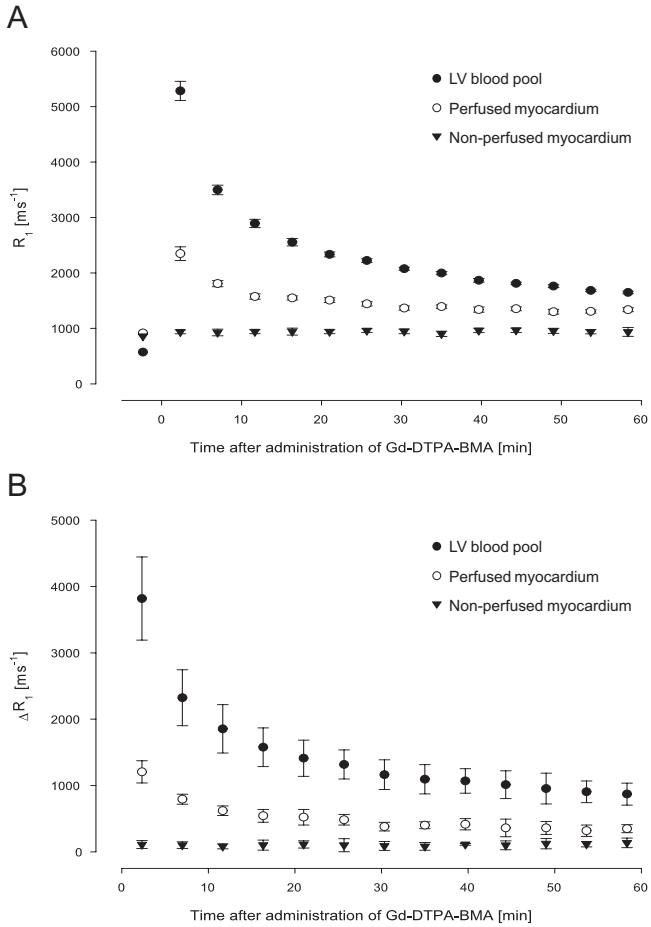

FIGURE 2 Relaxation rates (R_1) in blood pool, perfused myocardium, and nonperfused myocardium at baseline and during the first hour after CA administration. **a:** Example from one animal. R_1 increased rapidly in blood and perfused myocardium, but not in nonperfused myocardium. Error bars indicate the SDs of the measurements. **b:** ΔR_1 differed significantly between nonperfused myocardium and both blood and perfused myocardium during the first hour after CA administration. Error bars indicate 95 % CIs. $\Delta R_1 = R_{1,\text{time}} - R_{1,\text{baseline}}$.

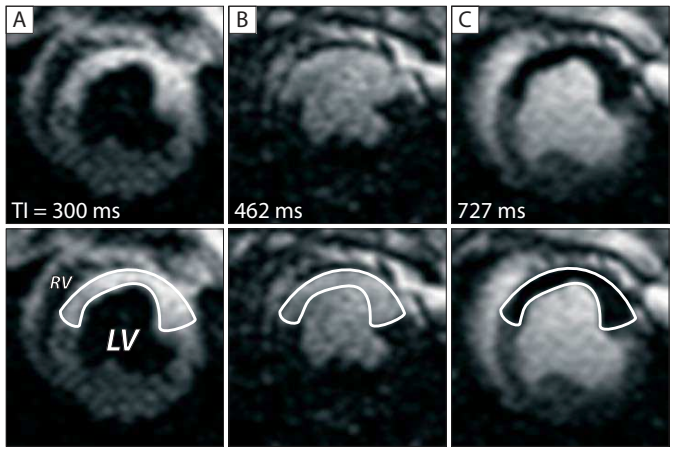

FIGURE 3 Short-axis image of the LV acquired 21 minutes after CA administration using a Look-Locker sequence consisting of 70 images. Three different TIs were chosen when the signal was nulled from blood (**a**), perfused myocardium (**b**), and nonperfused myocardium (**c**). The images correspond to the intensity bars in Figure 6B. The same images are shown without borders (upper row) and with nonperfused myocardium outlined (lower row). RV=right ventricle.

approximately 20–30 minutes after administration of CA[18] and in most instances within one hour. The small change in R_1 in the nonperfused myocardium directly after CA administration may be related to measurements close to the noise level of the image, or to contamination by pixels from the blood pool or viable myocardium with high R_1, since the image is acquired during the full cardiac cycle.

R_1 for nonperfused myocardium never reached the level of R_1 for perfused myocardium, and the two regions were quantitatively distinguishable for one hour after CA administration. It has been suggested that extracellular Gd-based CAs may diffuse into regions of low perfusion within one hour after administration.[9,15,17] Considering that diffusion is defined as a temperature- and concentration-dependent random three-dimensional walk by spontaneous movement, in accordance with thermodynamics,[22] the term diffusion may be misleading. Instead, it may be interstitial bulk flow driven by regional tissue pressure gradients that delivers the CA into nonperfused myocardium in vivo in the time span of less than one hour. It has also been shown that extracellular Gd-based CAs (ionic or nonionic) do not diffuse into ex vivo tissue homogenate of injured myocardium

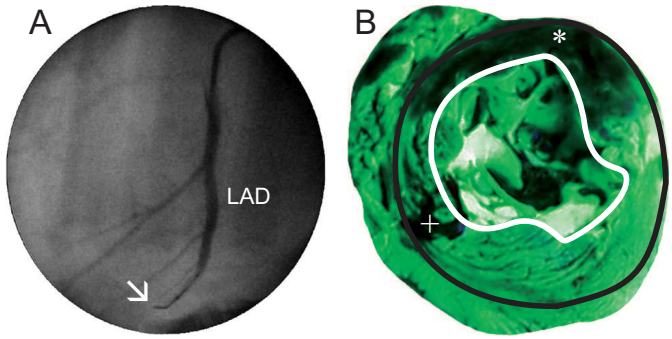

FIGURE 4 After MRI, persistent occlusion was verified by x-ray angiography and the nonperfused myocardium was delineated using fluorescein. **a:** Coronary angiogram illustrating occlusion of the LAD. Note the complete absence of blood flow distal to the occlusion (arrow). **b:** Fluorescein-stained slice under ultraviolet light, in which dark areas indicate nonperfused myocardium (*). LV endo- and eipcardial borders are indicated. Contamination by blood is indicated (+).

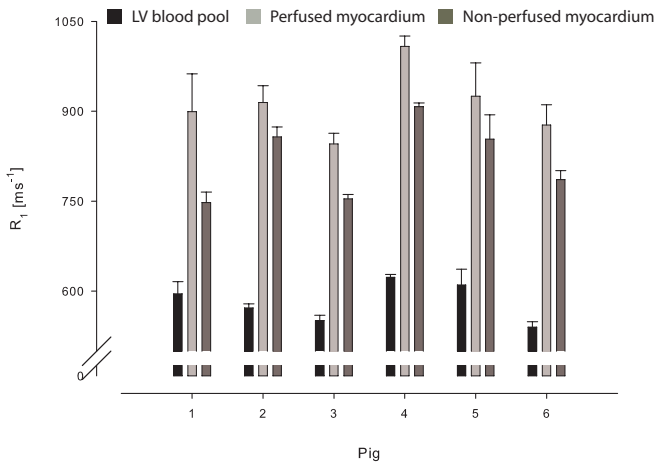

FIGURE 5 A difference in R_1 between blood (black), perfused myocardium (light grey), and nonperfused myocardium (dark grey) was found in all animals before CA administration. Error bars indicate SDs.

within one hour.[8] During the first hour after CA administration, we found no significant change in R_1 in the nonperfused myocardium in the in vivo, no-collateral flow model. This supports the notion that diffusion, even in the beating heart, is not sufficient to render "late enhancement" in nonperfused myocardium due to increased CA concentration within one hour after administration. The present results show that presence of flow (either vascular or interstitial bulk flow), as previously indicated,[5,10,13,19,21,30] is needed for delivery of extracellular Gd-based CAs. Contraction of viable perfused myocardium hypothetically may lead to higher CA transportation speed into nonperfused myocardiummyocardium; however, since we found no significant change in R_1 for the nonperfused myocardium, it is unlikely that contraction increases transportation of CA into nonperfused myocardium.

Figure 6 shows two principally different situations that can lead to higher signal intensity in injured myocardium after administration of an extracellular Gd-based CA. For clarity, fitted curves are presented as real data rather than measured magnitude data. Figure 6A shows a case in which the extracellular Gd-based CA had access to the injured myocardium. This region is enhanced due to a larger distribution volume of the CA,[1,18,24,28] and therefore relatively higher relaxation rate, compared to blood and viable perfused myocardium. However, if no CA enters the injured myocardium, the T_1 relaxation curves have a different appearance (Figure 6B). In the absence of CA the nonperfused myocardium (infarcted or not) is still hyperintense when the signal from perfused myocardium is nulled using an inversion recovery sequence (Figure 3B), since it is the magnitude of M_z and not the phase information that is used to present the viability image. Other factors, such as edema, may contribute to the intensity of nonperfused myocardium in magnitude images. In the current study, however, the relative changes in R_1 over time were measured and no changes were found, indicating that no CA enters nonperfused myocardium during the first hour after administration.

Phase information may be used for viability imaging,[16] and while it is not yet implemented as a standard for viability imaging, it may be offered as an option.

It is important to point out that the two situations described in Figure 6 also imply that intermediate levels of CA in injured myocardium may also occur. This region may thus be more or less indiscernible from blood or viable perfused myocardium. Factors that affect the presence of CA in a certain region include flow, distribution volume, and time after administration.

The presence of CA in injured myocardium is also an important factor for differentiating reversible from irreversible injury. This is because high signal intensity due to increased distribution volume requires loss of cellular integrity,[1] whereas high signal intensity due to the absence of CA in injured myocardium does not require loss of cellular integrity.

A possible limitation of this study is that the results may not be directly ap-

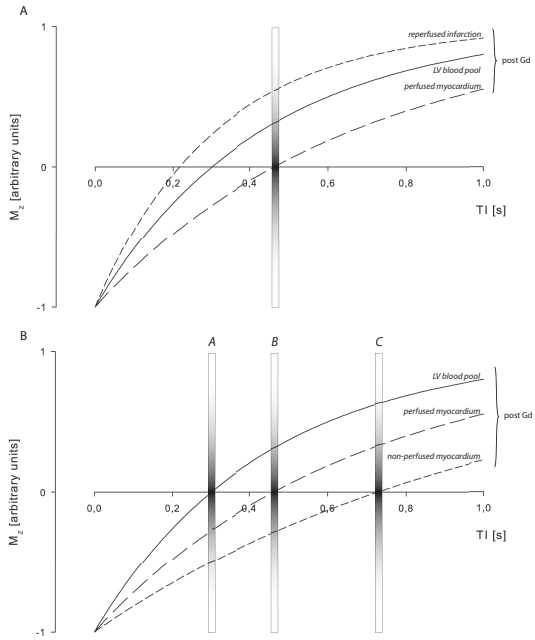

FIGURE 6 Two principally different situations that can lead to higher signal intensity in injured myocardium after administration of an extracellular Gd-based CA. Curves are derived from measured R_1 values 21 minutes after CA administration (see Materials and Methods), but are presented as real data for clarity. R_1 for reperfused infarction was adapted from unpublished results. **a:** Longitudinal magnetization recovery curves for the case in which the CA has access to the injured myocardium. This region is enhanced due to a larger distribution volume for CA.[1,18,24,28] **b:** Longitudinal magnetization recovery curves for the case in which the CA does not have access to the injured myocardium (as in the present study). Infarcted or not, in the absence of CA this region would still be hyperintense if the signal from perfused myocardium was nulled (c.f. Figure 3B). The signal intensity bars A, B, and C indicate nulling of the signal from blood, perfused myocardium, and nonperfused myocardium, respectively, and correspond to Figure 3a-c. M_z=magnetic moment in z-direction.

plicable to human studies, especially in the case of chronic ischemia, in which the collateral supply is increased, since the pig is known to have few if any collaterals.[2,26] However, the results may be relevant for acute ischemia without preconditioning or with insufficient reperfusion. A further limitation may be that images were acquired during a full cardiac cycle, and thus through-plane motion may have introduced an inflow component to R_1, which in combination with the low spatial resolution of the Look-Locker sequence may have influenced the measurements. However, we minimized that possibility by using a χ^2 error map. Also, the clearance of CA over the four minutes and 40 seconds of the Look-Locker acquisition may have affected the absolute quantification of R_1. These effects are likely small and systematic in nature, and therefore may have a limited impact on the relative changes in R_1 over time, as well as on our conclusions.

In conclusion, the present results show that Gd-DTPA-BMA does not enter ischemic myocardium within one hour after administration in acute coronary occlusion with no collateral flow. The ischemic region with complete absence of CA still appears bright when the signal from perfused myocardium is nulled using inversion recovery DE-MRI. This finding is important for understanding the basic pathophysiology of inversion recovery viability imaging, as well as for imaging of acute coronary syndroms.

Acknowledgments

The authors thank technicians Agneta Ronéus, Karin Fagerbrink, and Anne Abrahamsson for their help with animal preparation.

The study was funded by Swedish Research Council, Swedish Society of Medical Radiology, Lund University Medical Faculty, Heart Lung Foundation, and the Region of Scania.

References

1. H Arheden, M Saeed, CB Higgins, DW Gao, J Bremerich, R Wyttenbach, MW Dae, and MF Wendland. Measurement of the distribution volume of gadopentetate dimeglumine at echo-planar MR imaging to quantify myocardial infarction: comparison with 99mTc-DTPA autoradiography in rats. *Radiology*, 211(3):698–708, 1999.

2. T Bjerner, G Wikstrom, L Johansson, and H Ahlstrom. High in-plane resolution T2-weighted magnetic resonance imaging of acute myocardial ischemia in pigs using the intravascular contrast agent NC100150 injection. *Invest Radiol*, 39(8):470–8, 2004.

3. A Bjornerud, LO Johansson, K Briley-Saebo, and HK Ahlstrom. Assessment of T1 and T2* effects in vivo and ex vivo using iron oxide nanoparticles in steady state–dependence on blood volume and water exchange. *Magn Reson Med*, 47(3):461–71, 2002.

4. A Bjornerud, T Bjerner, LO Johansson, and HK Ahlstrom. Assessment of myocardial blood volume and water exchange: theoretical considerations and in vivo results. *Magn Reson Med*, 49 (5):828–37, 2003.

5. J Bremerich, MF Wendland, H Arheden, R Wyttenbach, DW Gao, JP Huberty, MW Dae, CB Higgins, and M Saeed. Microvascular injury in reperfused infarcted myocardium: noninvasive assessment with contrast-enhanced echoplanar magnetic resonance imaging. *J Am Coll Cardiol*, 32(3):787–93, 1998.

6. KM Choi, RJ Kim, G Gubernikoff, JD Vargas, M Parker, and RM Judd. Transmural extent of acute myocardial infarction predicts long-term improvement in contractile function. *Circulation*, 104(10):1101–7, 2001.

7. Look DC and D Locker. Time saving measurement of NMR and EPR relaxation times. *Rev Sci Instrum*, 41:250–251, 1970.

8. UK Decking, VM Pai, H Wen, and RS Balaban. Does binding of Gd-DTPA to myocardial tissue contribute to late enhancement in a model of acute myocardial infarction? *Magn Reson Med*, 49 (1):168–71, 2003.

9. P Dendale, PR Franken, M Meusel, R van der Geest, and A de Roos. Distinction between open and occluded infarct-related arteries using contrast-enhanced magnetic resonance imaging. *Am J Cardiol*, 80(3):334–6, 1997.

10. PW Doherty, MJ Lipton, WH Berninger, CG Skioldebrand, E Carlsson, and RW Redington. Detection and quantitation of myocardial infarction in vivo using transmission computed tomography. *Circulation*, 63(3):597–606, 1981.

11. MC Fishbein, S Meerbaum, J Rit, U Lando, K Kanmatsuse, JC Mercier, E Corday, and W Ganz. Early phase acute myocardial infarct size quantification: validation of the triphenyl tetrazolium chloride tissue enzyme staining technique. *Am Heart J*, 101(5):593–600, 1981.

12. SJ Flacke, SE Fischer, and CH Lorenz. Measurement of the gadopentetate dimeglumine partition coefficient in human myocardium in vivo: normal distribution and elevation in acute and chronic infarction. *Radiology*, 218(3):703–10, 2001.

13. CB Higgins, PL Hagen, JD Newell, WS Schmidt, and FH Haigler. Contrast enhancement of myocardial infarction: dependence on necrosis and residual blood flow and the relationship to distribution of scintigraphic imaging agents. *Circulation*, 65(4):739–46, 1982.

14. HB Hillenbrand, RJ Kim, MA Parker, DS Fieno, and RM Judd. Early assessment of myocardial salvage by contrast-enhanced magnetic resonance imaging. *Circulation*, 102(14):1678–83, 2000.

15. RM Judd, CH Lugo-Olivieri, M Arai, T Kondo, P Croisille, JA Lima, V Mohan, LC Becker, and EA Zerhouni. Physiological basis of myocardial contrast enhancement in fast magnetic resonance images of 2-day-old reperfused canine infarcts. *Circulation*, 92(7):1902–10, 1995.

16. P Kellman, AE Arai, ER McVeigh, and AH Aletras. Phase-sensitive inversion recovery for detecting myocardial infarction using gadolinium-delayed hyperenhancement. *Magn Reson Med*, 47 (2):372–83, 2002.

17. RJ Kim, EL Chen, JA Lima, and RM Judd. Myocardial Gd-DTPA kinetics determine MRI contrast enhancement and reflect the extent and severity of myocardial injury after acute reperfused infarction. *Circulation*, 94(12):3318–26, 1996.

18. C Klein, SG Nekolla, T Balbach, B Schnackenburg, E Nagel, E Fleck, and M Schwaiger. The influence of myocardial blood flow and volume of distribution on late Gd-DTPA kinetics in ischemic heart failure. *J Magn Reson Imaging*, 20(4):588, 2004.

19. T Masui, M Saeed, MF Wendland, and CB Higgins. Occlusive and reperfused myocardial infarcts: MR imaging differentiation with nonionic Gd-DTPA-BMA. *Radiology*, 181(1):77–83, 1991.

20. MT McNamara, D Tscholakoff, D Revel, R Soulen, N Schechtmann, E Botvinick, and CB Higgins. Differentiation of reversible and irreversible myocardial injury by MR imaging with and without gadolinium-DTPA. *Radiology*, 158(3):765–9, 1986.

21. S Nilsson, G Wikstrom, A Ericsson, M Wikstrom, A Waldenstrom, and A Hemmingsson. MR imaging of gadolinium-DTPA-BMA-enhanced reperfused and nonreperfused porcine myocardial infarction. *Acta Radiol*, 36(6):633–40, 1995.

22. F Reif. *Fundamentals of Statistical and Thermal Physics.* McGraw-Hill, New York, 1965.

23. M Saeed, MF Wendland, T Masui, and CB Higgins. Reperfused myocardial infarctions on T1- and susceptibility-enhanced MRI: evidence for loss of compartmentalization of contrast media. *Magn Reson Med*, 31(1):31–9, 1994.

24. J Schwitter, M Saeed, MF Wendland, N Derugin, E Canet, RC Brasch, and CB Higgins. Influence of severity of myocardial injury on distribution of macromolecules: extravascular versus intravascular gadolinium-based magnetic resonance contrast agents. *J Am Coll Cardiol*, 30(4): 1086–94, 1997.

25. OP Simonetti, RJ Kim, DS Fieno, HB Hillenbrand, E Wu, JM Bundy, JP Finn, and RM Judd. An improved MR imaging technique for the visualization of myocardial infarction. *Radiology*, 218(1):215–23, 2001.

26. PO Sjoquist, G Duker, and O Almgren. Distribution of the collateral blood flow at the lateral border of the ischemic myocardium after acute coronary occlusion in the pig and the dog. *Basic Res Cardiol*, 79(2):164–75, 1984.

27. P Storey, PG Danias, M Post, W Li, PR Seoane, PP Harnish, RR Edelman, and PV Prasad. Preliminary evaluation of EVP 1001-1: a new cardiac-specific magnetic resonance contrast agent with kinetics suitable for steady-state imaging of the ischemic heart. *Invest Radiol*, 38(10):642–52, 2003.

28. CY Tong, FS Prato, G Wisenberg, TY Lee, E Carroll, D Sandler, J Wills, and D Drost. Measurement of the extraction efficiency and distribution volume for Gd-DTPA in normal and diseased canine myocardium. *Magn Reson Med*, 30(3):337–46, 1993.

29. CM Wacker, F Wiesmann, M Bock, P Jakob, JJ Sandstede, A Lehning, G Ertl, LR Schad, A Haase, and WR Bauer. Determination of regional blood volume and intra-extracapillary water exchange in human myocardium using Feruglose: First clinical results in patients with coronary artery disease. *Magn Reson Med*, 47(5):1013–6, 2002.

30. KK Yu, M Saeed, MF Wendland, MW Dae, S Velasquez-Rocha, N Derugin, and CB Higgins. Comparison of T1-enhancing and magnetic susceptibility magnetic resonance contrast agents for demarcation of the jeopardy area in experimental myocardial infarction. *Invest Radiol*, 28(11): 1015–23, 1993.